Journal of Thermal Analysis and Calorimetry, Vol. 96 (2009) 2, 443–447

# DSC INVESTIGATIONS OF AMALGAM FORMATION IN Bi–Sn–Hg SYSTEM DOPED WITH INDIUM

*D. Janke*[1*], *J. Madarász*[1], *S. Lukács*[2] *and G. Pokol*[1]

[1]Department of Inorganic and Analytical Chemistry, Budapest University of Technology and Economics, 1521 Budapest, Hungary
[2]General Electric, Consumer and Industrial Lighting Technology, 1340 Budapest, Hungary

Differential scanning calorimetric (DSC) measurements have been carried out on Bi–Sn based amalgam precursors to be used in compact fluorescent lamps (CFLs) to study the changes in melting and solidifying behaviour caused by In dopant. The phase and elemental compositions of the samples have been characterized by using X-ray diffraction (XRD) and scanning electron microscopy–energy dispersive X-ray analysis (SEM-EDX), respectively. One of the endothermic peaks of the liquid amalgam formation shifted from 121°C to 112 and 105°C, with increasing content of 2.5 and 4.8 mass% In of samples, respectively.

***Keywords:*** *amalgam, DSC, fluorescent lamp, SEM-EDX, XRD*

## Introduction

Amalgams are used in compact fluorescent lamps (CFLs) to stabilise the mercury vapour pressure ($p_{Hg}$) inside the tube in a temperature ($T$) region, which ends at higher temperatures than that of lamps working with pure mercury. $p_{Hg}$–T characteristics of amalgams may go through a maximum and a minimum point, because of the simultaneous presence and phase equilibrium of solid and liquid phases. At the observed minimum the system gets completely molten, after which the mercury pressure begins rising again. This breakpoint temperature is lower than the eutectic or melting point of the amalgam forming subsystem. Furthermore in CFLs, liquid amalgam is formed during lamp operation and the mercury partial pressure above it is smaller than that of pure mercury at the actual temperature. In these ways the operating temperatures can be raised and the working temperature range can also be widened, compared to pure mercury.

The balance between mercury activation and reabsorption of ultraviolet radiation makes that an optimum $p_{Hg}$ is required. At this optimum the maximal output of visible light can be achieved. The optimum $p_{Hg}$ is typically 1–2 Pa for CFLs [1, 2], which of course belongs to the maximum of light output. The lamp amalgam precursors get molten during lamp operation. The stabilization in mercury vapour pressure is only present in the temperature region between the melting of the phase with the lowest melting point and the temperature of the complete melting of the amalgam forming system. For that very reason it is important to know at which temperatures the different constituent phases melt. By knowing this information we have a chance to predict the behaviour of amalgams as a function of temperature.

Differential thermal analysis (DTA) and DSC are commonly used techniques to examine the thermal behaviour of alloys or metallic mixtures and also to establish phase diagrams. Lankhorst *et al*. [2] have used DTA to examine and compare the $Bi_{0.56}Pb_{0.44}$, the $Bi_{0.55}Pb_{0.43}Au_{0.02}$ and the $Bi_{0.5}Pb_{0.4}Au_{0.1}$ mixtures and DSC to find out how many crystalline phases $BiPb_3Au$ could contain. Using DSC, Herda *et al*. [3] studied the effects on the thermal behaviour of a lathe-cut type of high copper amalgam by the addition of a small amount of palladium. El-Hadary *et al*. [4] have used DSC to differentiate between the $Hg_3Ag_2$ and the $Sn_{7-8}Hg$ phases in four different types of dental amalgams. Vassiliev *et al*. [5] also used DTA to investigate a part of the Ag–Bi–In ternary system. Souza *et al.*[6] have used DSC and other analytical techniques to study the reaction of mercury with platinum foils and to identify the possible formation of intermetallic compounds. Witusiewicz *et al.* [7] measured the phase transformations and the enthalpy of melting of 29 different alloys from the Bi–In–Sn system to optimize the phase diagram of the system.

To stabilise the mercury vapour pressure it is necessary to have an appropriate amalgam forming system, which melts in the required temperature region and which retains its mercury vapour pressure compared to the pressure of pure mercury. A number of lower melting metals had been studied that have reasonably low vapour pressures i.e. In, Bi, Pb, Sn and Ga. Some others are unsuitable for putting into production, because of their toxicity, such as Cd and Tl.

* Author for correspondence: denes.janke@gmail.com

1388–6150/$20.00
© 2009 Akadémiai Kiadó, Budapest
Akadémiai Kiadó, Budapest, Hungary
Springer, Dordrecht, The Netherlands

From the Bi–Sn–Pb ternary system, the amalgam formed with the eutectic metallic mixture $Bi_{0.44}Sn_{0.27}Pb_{0.29}$, [melting point of 100°C [1] was found to be very good at room temperature as well as at working temperature [8]. Because of an EU-directive [9] Pb can not be used anymore in electrical and electronic equipment, so we have to find new melting point-lowering additives to get good amalgams like the $Bi_{0.45}Sn_{0.23}Pb_{0.26}Hg_{0.06}$ and the $Bi_{0.47}Sn_{0.23}Pb_{0.27}Hg_{0.03}$ amalgams [10]. Bi–In–Hg is a widespread substitute for the Bi–Sn–Pb–Hg amalgams. During the detailed studies of the Bi–In system, Evans *et al*. [11] have set up the phase diagram of the Bi–In system. According to both Evans *et al*. [11] and Vassiliev *et al*. [5] the eutectic mixture of Bi and the BiIn intermetallic compound ($Bi_{0.53}In_{0.47}$) melts at 109.7°C, but this amalgam precursor is only suitable for traditional, non-covered CFLs and not for covered, décor lamps. For décor lamps Bi–Sn–Hg amalgams seem to be suitable, because of the eutectic melting point of 139°C of the eutectic $Bi_{0.43}Sn_{0.57}$, which system was studied by Ishihara *et al*. [12] and by Nosek *et al*. [13].

The In–Hg amalgam with 6 mass% Hg was found to be a useful mercury source [8, 14]. Coles *et al*. [15] and Kozin *et al*. [16] have examined the In–Hg system. The melting point of the In–Hg system is beneath the melting point of pure In at 157°C. On the other hand, studies of Dinsdale *et al*. [17] have shown that in the case of the Bi–Hg amalgam, in solid phase Bi does not intermingle with mercury at all. Zabdyr *et al*. have collected detailed bibliographic data concerning the phase diagrams of the Sn–Hg [18] and the Bi–Hg [19] systems. Yen *et al*. [20] have made a thermodynamic assessment of the Sn–Hg system using the CALPHAD method. Using this method, they found a reasonable agreement with the phase diagram made up of measured data. The vapour pressure and enthalpy data of both Hg and Sn in liquid Hg–Sn alloys above about 177°C were also in very good agreement with literature data.

Our effort was to seek lead substituting additives to decrease the eutectic melting point of the Bi–Sn system. For this reason we have examined the thermal behaviour of the indium doped Bi–Sn system. Although it is in the high In content area, as reported by Stel'makh *et al*. [21], the ternary eutectic alloy of the Bi–In–Sn system with the composition of $Bi_{0.204}In_{0.573}Sn_{0.223}$ had a eutectic temperature of 59°C.

The DSC analyses of low indium content samples have been carried out in order to get a dynamic picture of the occurring heat effects as a function of temperature during the heating and the cooling phase of the amalgam forming samples. The SEM-EDX analyses to characterize the composition of the samples and the XRD analyses were carried out to identify the phases which occur in the initial and the re-cooled samples.

## Experimental

### *Samples*

Three different ball-shaped amalgam samples from system Bi–Sn–In–Hg have been studied, marked as samples 1, 2 and 3. Samples 1–3 used for the DSC measurements had a mass of 35.028, 62.584 and 70.515 mg, respectively. The outer appearance of the three samples was very similar. They differed from each other in their mass and diameter. All of them had a matt, metallic coloured surface. The samples were hard, so for the XRD and SEM-EDX measurements they were flattened between alumina flans to get a larger examination surface. After the flattening the samples have lost their matt surface and became glossy.

### *Methods*

#### Differential scanning calorimetry (DSC)

The differential scanning calorimetric measurements were carried out on a DSC 2920 (TA Instrument) apparatus. The samples were placed in a hermetically sealed aluminium crucible. As a reference we used a similar but empty aluminium crucible. The amalgam samples were heated at a rate of 3°C $min^{-1}$ to 150°C, the heating was turned off during the cooling phase.

#### Scanning electron microscopy-energy dispersive X-ray analysis (SEM-EDX)

Scanning electron microscopy and energy dispersive X-ray emission measurements were carried out on a JEOL JSM-5500LV Scanning Electron Microscope instrument. During the measurements we used accelerating voltages of $U$=20 and 30 kV. Composition of the samples were measured with semiconductor Si(Li) detector cooled with liquid nitrogen and calculated by using the evaluating IXRF EDS 2000 (Version 3.1. Rev.D.) software of the EDX instrument. The morphological and compositional images were captured both with a secondary electron imaging (SEI) and a back-scattered electron imaging (BSI) detector.

#### X-ray diffraction (XRD)

The X-ray diffraction measurements were carried out on an X'Pert PRO MPD diffractometer (PANalytical). The measurements were made at room temperature in θ–θ mode. The flattened samples were placed on a zero-background Si single crystal sample holder. X-ray profiles were measured between 5–85° (2θ) with automatic divergence slit of 15 mm and with a fixed anti-scatter slit of 1° and a mask size of 15 mm. We used the $CuK_\alpha$ line (λ=1.5408 Å, $U$=40 kV; $I$=30 mA)

filtered by a Ni foil (0.02 mm thick) and an X'-celerator detector in scanning mode. The identification of the phases was carried out with the X'Pert High Score Plus program's Search-Match algorithm based on the ICDD PDF-2 database [22].

## Results and discussion

*Characterisation of samples*

Elemental composition of samples

The samples' compositions have been determined by the characteristic X-ray emission spectra at a magnification of 50×. The average semi-quantitative compositions of the three amalgam samples can be seen in Table 1. Sample 1 did not contain In at all. Sample 3 contained approximately double as much In as sample 2 did.

**Table 1** Elementary of samples composition 1–3 in mass%, measured with SEM-EDX semi-quantitatively

| Element | Sample 1 | Sample 2 | Sample 3 |
|---|---|---|---|
| Bi | 40.19 | 44.64 | 35.17 |
| Sn | 49.24 | 47.18 | 56.14 |
| Hg | 10.55 | 5.65 | 3.88 |
| In | 0.00 | 2.51 | 4.79 |

Phase composition of samples

Based upon the X-ray diffraction patterns we could identify two crystalline phases with XRD in sample 1, such as Bi metal (PDF 01-071-4642 [22, 23]) and γ-$Sn_xHg$ ($x$=6–12) (PDF 03-065-6776 or PDF 00-048-1546 [22, 24, 25]). In the samples 2 and 3, we could identify metallic Bi (PDF 01-071-4642 or 01-071-4643 [22, 23, 26]), γ-$Sn_xHg$ ($x$=6–12) (PDF 03-065-6776 or 00-048-1546 [22, 24, 25]) and Sn metal (PDF 01-086-2264 or 00-004-0673 [22, 27]). We could not identify the crystalline phase with In content in samples 2 and 3. This can be due to the fact that the XRD pattern of $Sn_4In$ (PDF 00-048-1547 [22, 25]) is very similar to the pattern of the γ-$Sn_xHg$ ($x$=6–12) phase [25].

*DSC studies*

During the heating run of sample 1 (Fig. 1, bottom curve), the amalgam shows a slight elongated endothermic effect centred at 76°C, followed by the endothermic melting peak at 121°C, which seems to be superposed on a wider endothermic melting peak centred at 125°C (Table 2). According to Nosek *et al*. [13] at 76°C liquid mercury is released from the γ-$Sn_xHg$ phase. This is followed by the dissolution of the

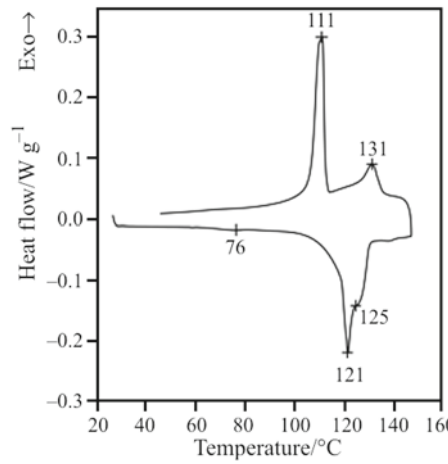


**Fig. 1** DSC curve of Bi–Sn–Hg amalgam free from In (sample 1, mass 35.028 mg). The bottom curve marks the heating run and the top curve marks the cooling run of sample 1

γ-$Sn_xHg$ phase into liquid mercury at 121°C. Finally, the Bi metal phase slowly dissolves at 125°C, and the sample gets totally molten. The peak temperatures of the heating run of samples 1–3 can be found in Table 2. During the cooling phase supercooling was observed.

During the cooling run of sample 1 (Fig. 1, top curve), the amalgam showed two exothermic effects centred at 131 and 111°C. The peak at 131°C can be assigned to the crystallisation of Bi and the peak at 111°C can be assigned to the crystallisation of the γ-$Sn_xHg$ phase. The peak temperatures of the cooling run of samples 1–3 can be found in Table 3.

During the DSC measurements of the samples 2 and 3, we experienced a similar melting (Fig. 2, bot-

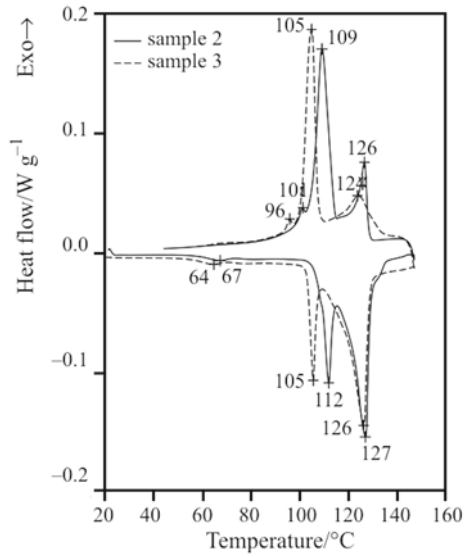


**Fig. 2** DSC curve of Bi–Sn–In–Hg amalgams, with 2.5 (sample 2, mass 62.584 mg) and 4.8 (sample 3, 70.515 mg) mass% In. The bottom curves mark the heating runs and the top curves mark the cooling runs of samples 2 and 3

**Table 2** Peak temperatures during the heating run of the DSC measurements

| Heating | In/mass% | Centre of temperature range of Hg release/°C | Peak temperature of dissolution $Sn_xHg$ and/or $Sn_4In$/°C | Final temperature of Bi dissolution/°C |
|---|---|---|---|---|
| Sample 1 | 0.0 | 76 | 121 | 125 |
| Sample 2 | 2.5 | 67 | 112 | 127 |
| Sample 3 | 4.8 | 64 | 105 | 126 |

**Table 3** Peak temperatures during the cooling run of the DSC measurements

| Cooling | In/mass% | Crystallisation of Bi/°C | Crystallisation of $Sn_xHg$/°C | Crystallisation of $Sn_4In$/°C |
|---|---|---|---|---|
| Sample 1 | 0.0 | 131 | 111 | – |
| Sample 2 | 2.5 | 126 | 109 | 101 |
| Sample 3 | 4.8 | 124 | 105 | 96 |

tom curves) and solidifying (Fig. 2, top curves) behaviour compared to that of sample 1. Both samples 2 and 3 released liquid mercury in a temperature range approximately 10°C lower than sample 1 did. In the DSC curve of both samples 2 and 3, the endothermic melting peak at 126 and 127°C remained close to the endothermic melting peak of sample 1 at 125°C, but the endothermic melting peak of 121°C shifted to lower temperatures (Table 2). In addition, the shift got even larger with increasing In content, as it can be seen in Fig. 2 on the DSC curve of sample 3 which had a higher In content and as a result of that, it produced an endothermic melting peak already at 105 instead of 121°C, where sample 1 did. During the cooling phase of the measurement, a small additional exotherm peak of solidifying emerged at 101°C for sample 2 and at 96°C for sample 3 which contained the higher amount of In (Table 3).

After the DSC measurements, we checked the samples' phase composition again with XRD. Sample 1 did not show any changes. However, after heating samples 2 and 3 up to 150°C, we could not detect the presence of the Sn phase in either of the samples. Only the Bi and the γ-$Sn_xHg$ (probably together with the very similar $Sn_4In$) phases remained in samples 2 and 3 after the DSC heating.

## Acknowledgements

The authors wish to thank Dr. Béla Koczka and Mr. Imre Miklós Szilágyi for their help in the SEM-EDX measurements and Mrs. E. Tóth for her help in the DSC measurements. The authors also thank for the purchase grant of new HT-XRD apparatus supported by the EU and Hungarian goverment (GVOD-3.2.1.-2004-4-0224, KMA). The kind and useful help as private communication from Dr. Stuart Mucklejohn is gratefully acknowledged.

## References

1 M. H. R. Lankhorst and U. Niemann, J. Alloys Compd., 308 (2000) 280.
2 M. H. R. Lankhorst, W. Keur and H. A. M. van Hal, J. Alloys Compd., 309 (2000) 188.
3 E. Herda and R. H. R. Parangtopo, Mater. Lett., 30 (1997) 347.
4 M. S. El-Hadary, A. Kamar, A. Fayed, A. S. El-Kady, S. H. Kandil and S. E. Morsi, J. Thermal Anal., 29 (1984) 131.
5 V. Vassiliev, M. Alaoui-Elbelghiti, A. Zrineh, M. Gambino and J. P. Bros, J. Alloys Compd., 265 (1998) 160.
6 G. R. Souza, I. A. Pastre, A. V. Benedetti C. A. Ribeiro and F. L. Fertonani, J. Therm Anal. Cal., 88 (2007) 127.
7 V. T. Witusiewicz, U. Hecht, B. Böttger and S. Rex, J. Alloys Compd., 428 (2007) 115.
8 J. Bloem, A. Bouwknegt and G. A. Wesselink, J. Illum. Eng. Soc., 6 (1977) 141.
9 Directive 2002/95/EC of the European Parliament and of the council of 27 January 2003 on the restriction of the use of certain hazardous substances in electrical and electronic equipment.
10 U.S. Patent No. 4,093,889, Assignee: U.S. Philips Corporation, New York, N.Y. Filed: 1977.
11 D. S. Evans and A. Prince, Metal Sci., 17 (1983) 117.
12 K. N. Ishihara, M. Maeda, K. Mori and P. H. Shingu, Int. J. Rapid Solidif., 3 (1987) 11.
13 M. V. Nosek, N. M. Semivratova and G. V. Yan-Sho-Syan, Izv. Akad. Nauk SSSR Metally, 1 (1970) 178.
14 U.S. Patent No. 3,619,697, Assignee: Westinghouse Electric Corporation, Pittsburgh, Pa., Filed: 1964.
15 B. R. Coles, M. F. Merriam and Z. Fisk, J. Less Common Metals, 5 (1963) 41.
16 L. F. Kozin and V. A. Sudakov, Izv. Akad. Nauk SSSR Met., 5 (1970) 197.
17 A. T. Dinsdale, G. M. Forsdyke and S. A. Mucklejohn, Proc. 9th International Conference in High Temperature Materials Chemistry, (1997) 44.
18 L. A. Zabdyr and C. Guminski, J. Phase Equilibria, 14 (1993) 743.
19 L. A. Zabdyr and C. Guminski, J. Phase Equilibria, 17 (1996) 230.

20 Y. W. Yen, J. Gröbner, S. C. Hansen and R. Schmid-Fetzer, J. Phase Equilib., 24 (2003) 151.
21 S. I. Stel'makh, V. A. Tsimmergall and J. A. Sheka, Ukr. Khim. Zh., 38 (1972) 855.
22 The International Centre for Diffraction Data, Powder Diffraction File-2 database, (Release 2007).
23 H. Kahler, Phys. Rev., 18 (1921) 210.
24 T. F. Grigorjeva, E. Yu. Ivanov, V. V. Boldyrev, E. I. Petrachkov and T. I. Samsonova, Izv. Sib. Otd. Akad. Nauk SSSR, Ser. Khim. Nauk, 4 (1989) 46.
25 G. C. Che, M. Ellmer and K. Schubert, J. Mater. Sci., 26 (1991) 2417.
26 W. P. Davey, Philos. Mag., 47 (1924) 657.
27 H. E. Swanson and E. Tatge, Natl. Bur. Stand. (U.S.), 1 (1953) 539.

Received: July 17, 2008
Accepted: September 30, 2008
Online First: February 4, 2009

DOI: 10.1007/s10973-008-9426-z